3D Radiative Hydrodynamics Modeling of Convection of Stars to Probe Their Interiors and Photospheric Properties

Irina Kitiashvili, NASA Ames Research Center

The dramatic flow of data from the Kepler and K2 missions opens the opportunity to significantly improve our knowledge of stellar interiors, surface dynamics, and structure. However, interpretation of these observations is a challenging task because it depends on tiny effects that can be studied only with advanced first-principles modeling. We present results of 3D time-dependent radiative hydrodynamic simulations of stellar outer convection zones and atmospheres taking into account chemical composition, radiative transfer, turbulence effects, and a realistic equation of state for main-sequence stars. We will discuss properties of convective structure and dynamics, convective overshoot, effects of magnetic fields and rotation, as well as the potential influence of turbulent surface dynamics on high-precision RV measurements.

'StellarBox' code (Wray et al., 2018)

- ✓ 3D rectangular geometry
- ✓ Fully conservative compressible MHD
- ✓ Fully coupled radiation solver:
  - LTE using 4 opacity-distribution-function bins
  - Ray-tracing transport by Feautrier method
  - 18 ray (2 vertical, 16 slanted) angular quadrature
- ✓ Non-ideal (tabular) EOS
- ✓ 4th order Padé spatial derivatives
- ✓ 4th order Runge-Kutta in time
- ✓ LES-Eddy Simulation options (turbulence models):
  - LES: Smagorinsky model (and its dynamic procedure)
  - DNS + Hyperviscosity approach
  - MHD subgrid turbulence models

Basic equations

The equations we solve are the grid-cell averaged

Conservation of mass:
$$\frac{\partial \rho}{\partial t} + (\rho u_i)_{,i} = 0$$

Conservation of momentum:
$$\frac{\partial \rho u_i}{\partial t} + (\rho u_i u_j + P_{ij})_{,j} = -\rho \phi_{,i}$$
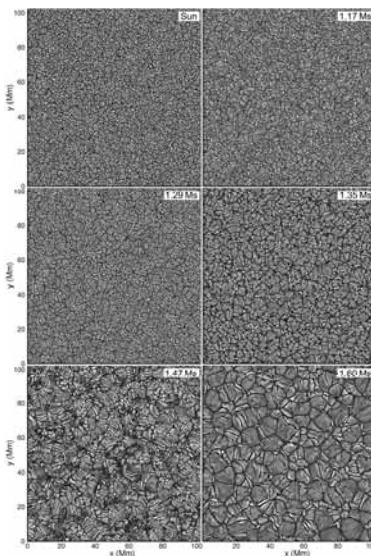
Conservation of energy:
$$\frac{\partial E}{\partial t} + \left(\begin{array}{l} E u_i + P_{ij} u_j - \kappa T_{,j} + \\ + \left(\frac{c}{4\pi}\right)^2 \frac{1}{\sigma}(B_{i,j} - B_{j,i})B_j + F_i^{rad} \end{array} \right)_{,j} = 0$$
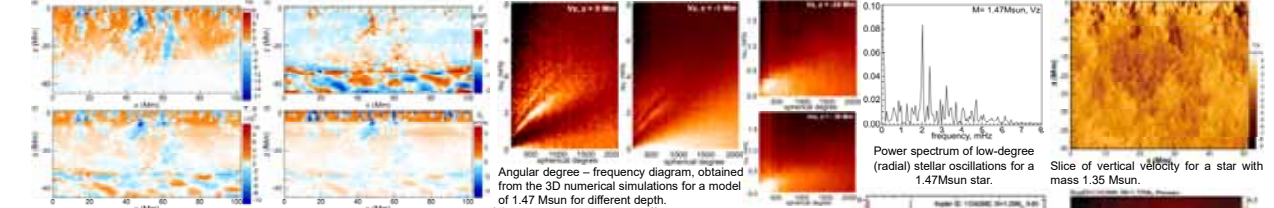
with
$$P_{ij} = \left(p + \frac{2}{3}\mu u_{k,k} + \frac{1}{8\pi}B_k B_k\right)\delta_{ij} - \mu(u_{i,j} + u_{j,i}) - \frac{1}{4\pi}B_i B_j$$

Conservation of magnetic flux
$$\frac{\partial B_i}{\partial t} + \left(u_j B_i - u_i B_j - \frac{c^2}{4\pi\sigma}(B_{i,j} - B_{j,i})\right)_{,j} = 0$$

Vertical slice for the modeled star (1.47M_{sun}) shows: a) vertical velocity, b) density, c) temperature, and d) sound speed perturbations from the radiative zone to the stellar photosphere. Large-scale density fluctuations in the radiative zone are caused by internal gravity waves (g-modes) excited by convective overshooting. Depth z is defined as: z=r-R.
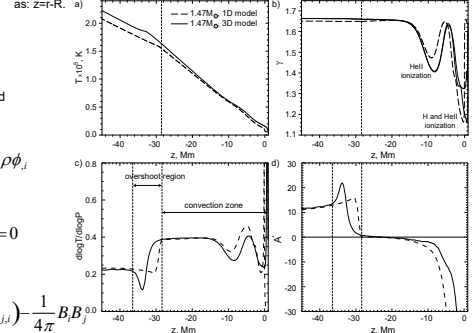
Comparison of the 1D interior structure of a moderate mass star (M=1.47M_{sun}) calculated using mixing-length theory (dashed curves) and from the 3D simulation (solid curves): a) temperature; b) adiabatic exponent; c) temperature gradient; d) Ledoux parameter of convective stability, A*. Vertical dotted lines indicate the bottom of the convection zone and the extent of the overshoot region in the 3D simulation. The mean profiles of the simulation are calculated by averaging in the horizontal directions and over a 1 hour interval. The thin curve in panel b) shows the value of the adiabatic exponent calculated from the mean density and internal energy profiles of the 3D model (Kitiashvili et. al. 2016).
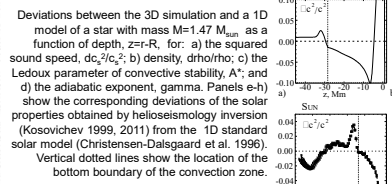
Deviations between the 3D simulation and a 1D model of a star with mass M=1.47 M_{sun} as a function of depth, z=r-R, for: a) the squared sound speed, dc_s^2/c_s^2; b) density, drho/rho; c) the Ledoux parameter of convective stability, A*; and d) the adiabatic exponent, gamma. Panels e-h) show the corresponding deviations of the solar properties obtained by helioseismology inversion (Kosovichev 1999, 2011) from the 1D standard solar model (Christensen-Dalsgaard et al. 1996). Vertical dotted lines show the location of the bottom boundary of the convection zone.

Variation in the scales of granulation for different main-sequence stars with increasing stellar mass. Distribution of the vertical velocity is saturated for range +/- 6 km/s.
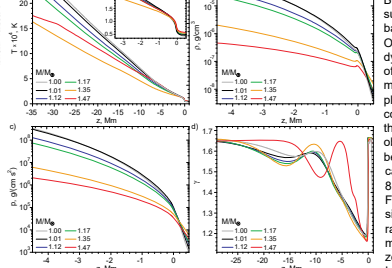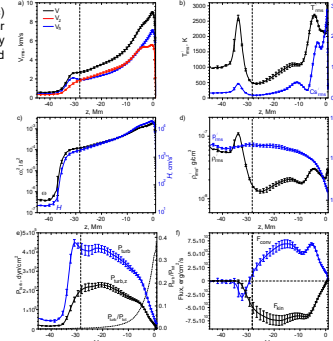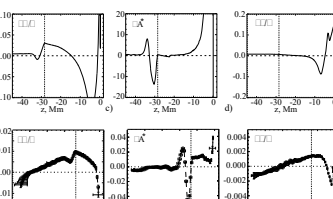
Models of interior structure of the stars obtained with a stellar evolution code.

Angular degree – frequency diagram, obtained from the 3D numerical simulations for a model of 1.47 Msun for different depth.
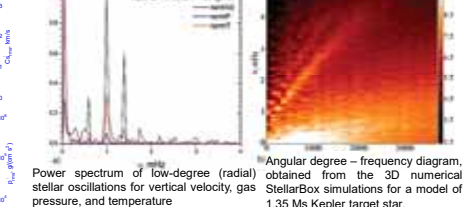
Vertical profiles, obtained from the 3D numerical simulation of a 1.47Msun F-type star (Kitiashvili et. al. 2016): a) rms of velocity V (black), vertical Vz (red) and horizontal Vh (blue) components of velocity; b) rms of temperature T' (black) and sound speed c_s' (blue) perturbations; c) entrophy (black) and helicity H (blue); d) rms of density (black) and gas pressure P' (blue) perturbations; e) turbulent P_{turb} (blue curve), turbulent pressure of the vertical motions P_{turb} (black), and the ratio of turbulent pressure P_{turb} to total pressure $P_{turb}+P$; and f) convective energy flux F_{conv} (blue curve) and kinetic energy flux F_{kin} (black), calculated according to the formulation of Nordlund & Stein (2001). Vertical dashed lines indicate the bottom boundary of the convection zone of the corresponding 1D stellar model: z_{cz}=-28.5 Mm.

Power spectrum of low-degree (radial) stellar oscillations for a 1.47Msun star.

Slice of vertical velocity for a star with mass 1.35 Msun.

Power spectrum of low-degree (radial) stellar oscillations for vertical velocity, gas pressure, and temperature

Angular degree – frequency diagram, obtained from the 3D numerical StellarBox simulations for a model of 1.35 Ms Kepler target star.

Effects of rotation

M = 1.47 M_{sun}, P_{rot} = 1day

Vertical distribution of the velocity components for two rotation rates (P_{rot} = 1 day and 14 days) and 3 latitudes: 0 deg (equator), 30 deg and 60 deg. The vertical velocity profiles are averaged over 1 hour.
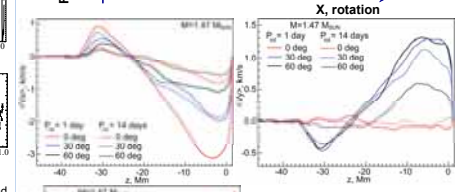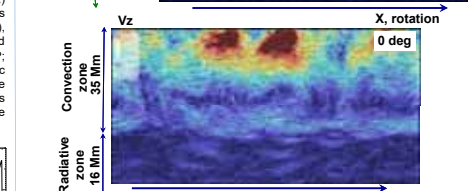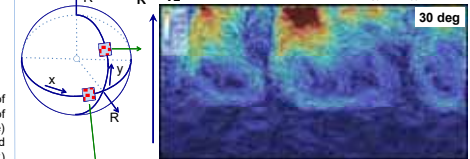
Conclusions

Because of complexity of the physics of stellar surface and subsurface layers, 'ab initio' (or 'realistic'), numerical simulations based on first principles are a primary tool of theoretical modeling.

Our investigation of main-sequence stars has shown that the dynamics of stellar convection dramatically changes among stars of different masses. The convection zone is shallower for more massive stars, turbulent convection becomes more vigorous, with plasma motions reaching supersonic speeds and multi-scale convective cell structures appearing that can be quite different from the granulation and supergranulation known from solar observations. Convective downdrafts in intergranular lanes between granulation clusters reach speeds of more than 20km/s, can penetrate through the whole convection zone and hit the radiative zone, and form a 8Mm thick overshoot layer.

For stars with M > 1.35Ms the convection zone is relatively shallow, and high-resolution simulation domains cover its entire depth, including a convectively stable layer of the radiative zone. This allows us to investigate the physics of overshooting and turbulent mixing, as well as excitation of internal gravity waves at the bottom of the convection zone.

Including the effects of rotation reveals formation of roll-like structures at the bottom of the convection zone that lead to the development of anti-solar differential rotation for a star of 1.47 solar mass.

References

Christensen-Dalsgaard J. et al. 1996. Science 272, 1286.
Kitiashvili I. N. et. al. 2016. ApJ 821, article id. L17, 8.
Kosovichev A. G. 1999. J. Comput. Appl. Math., 109, 1.
Kosovichev A. G. 2011. In Lecture Notes in Physics, Vol. 832. Berlin: Springer, 3-84.
Nordlund A. & Stein R. F. 2001. ApJ 546, 576
Wray A. A. et al. 2018. Realistic simulations of Stellar Radiative MHD. In Book: "Variability of the Sun and Sun-like Stars: from Asteroseismology to Space Weather". EDP Sciences, 2018. p.39-62. ArXiv:1507.07999